IJP: Parasites and Wildlife 10 (2019) 289–298

Contents lists available at ScienceDirect

IJP: Parasites and Wildlife

journal homepage: www.elsevier.com/locate/ijppaw

Morphological and molecular identification of epibiontic sessilid *Epistylis semiciculus* n. sp. (ciliophora, Peritrichia) from *Procambarus clarkia* (Crustacea, Decapoda) in China

Tong Zhou[a,b], Zhe Wang[a,b], Hao Yang[a,b], Zemao Gu[a,b,*]

[a] Department of Aquatic Animal Medicine, College of Fisheries, Huazhong Agricultural University, Wuhan, 430070, PR China
[b] Hubei Engineering Technology Research Center for Aquatic Animal Diseases Control and Prevention, Wuhan, 430070, PR China

ARTICLE INFO

Keywords:
Morphological characteristics
Phylogenetic analyses
SSU rDNA sequences
Intraspecific morphological variation
Crustacean

ABSTRACT

Data on sessilinasis from *Procambarus clarkia* are limited. This study investigates sessilid diversity in Hubei Province, China in 2016. *Procambarus clarkia* pereopods were covered by two sessilid morphotypes in April and May, and the gills were adhered by one of these two morphotypes (morphotype I) in January. Identifying the two morphotypes according to their morphological characters through live observations and protargol-stained method is difficult. Both morphotypes show almost identical morphological characteristics: zooids present vase-shaped, the length-to-width ratio is 2:1, the semicircle-shaped peristomial disk is evidently above the peristomial lip, single contractile vacuole is located below the peristomial lip, and the oral infraciliature shows identical arrangement which can be distinguished from other *Epistylis*. However, the morphometric data of the two morphotypes are significant different: body size of morphotype I is 78.9–103.8 × 32.1–54.6 μm, whereas that of morphotypes II is 136.7–171.5 × 60.9–88.0 μm. To further identify the two morphotypes, molecular regions including small subunit ribosomal DNA (SSU rDNA) sequences, large subunit ribosomal DNA (LSU rDNA) sequences, and ITS1-5.8S-ITS2 sequences were used. Results supported that the two morphotypes are single species of genus *Epistylis* rather than distinct species based in their distinct size ranges and temporal presence events. We assigned it the name *E. semiciculus* n. sp. with respect to the semicircular peristomial disk. Overall, these findings emphasized the importance of using molecular data to solve the identification confusion caused by ontogenetic processes. This study is the first morphological and molecular characterization of a sessilid isolated from *P. clarkia* under aquaculture conditions.

1. Introduction

Red swamp crayfish, *Procambarus clarkia* is a high-quality source of protein for human and plays an increasingly important role in world-wide aquaculture for global food supplying (FAO, 2018). *Procambarus clarkia* was artificially cultured in the United States at 1950's decade (Hobbs, 1989; Gherardi, 2006). In the 1990s, *P. clarkia* culture started to be highly valued in China (Chen et al., 2008). Currently, the *P. clarkia* accounts for the largest part of the freshwater crustacean aquaculture in China, as *P. clarkia* production reached 1,129,708 tons in 2017 (Xu and Lv, 2018). With the rapid development of intensive culture, the risk of infectious diseases of *P. clarkia* has increased, resulting in so far unknown economic losses (Van and Viljoen, 1984; Overstreet, 1987; Pádua et al., 2013; Wang et al., 2017b).

One of the most common diseases is caused by sessilids that belong to a highly diversified group of peritrichs. The order Sessilida Kahl, 1933 is characterized by a trophont stage attached onto a substrate through a lorica, scopula, or stalk (Lynn, 2008). Sessilid identification was traditionally based on morphological methods that use in vivo observation, protargol staining, and electron microscopy (Lynn, 2008). Molecular identification methods were used to validate traditional taxonomy which been under debate. Numerous morphological characteristics used to distinguish families or species have been queried by recent molecular studies (Utz et al., 2010; Sun et al., 2012; Jiang et al., 2016). However, revising a proper taxonomy is difficult because of lacking corresponding molecular data (Lynn, 2008; Gao et al., 2017). Sessilids can firmly stick to the gill and the exoskeleton of crustacean via the stalk (Hunn, 1966; Villarreala and Hutchingsb, 1986). The attachment of sessilids may result in tissues necrosis, respiratory retardation and mortality for crustaceans (Villarreala, 1986). Despite their potential impact on crustaceans, reserch on therapeutic treatment of sessilinasis is still at an early stage because sessilids have different

* Corresponding author. Huazhong Agricultural University, No.1, Shizishan Street, Hongshan District, Wuhan, 430070, PR China.
E-mail address: guzemao@mail.hzau.edu.cn (Z. Gu).

https://doi.org/10.1016/j.ijppaw.2019.09.006
Received 6 March 2019; Received in revised form 21 September 2019; Accepted 21 September 2019

sensitivities to drug and preferences for adhesion sites (Van, 1984; Vogelbein and Thune, 1988; López-Téllez et al., 2009; Wang et al., 2016). Thus, taxonomic identification of sessilids on crustacean is required for research on resistance to aquaculture disease.

This study aimed to provide insights into the diagnosis of potential pathogens for crustacean and taxonomic revision for sessilids by describing two morphotypes of sessilid ciliates isolated from *Procambarus clarkia*. Morphotype I and morphotype II adhered onto the pereopods in April and May, whereas morphotype I adhered onto the gills in January. Morphological characteristics based on in vivo specimens and silver protargol staining, as well as the results of phylogenetic analyses based on SSU rDNA sequences and ITS1-5.8S-ITS2 sequences, were provided. Both morphotypes were identified as conspecific of a new species of *Epistylis* Ehrenbeg (1830) based on almost morphological characteristics and molecular data, although the size ranges are distinct. This work provided the first and the most comprehensive record on sessilids isolated from *P. clarkia* and strengthened the importance of molecular data used in species identification.

2. Materials and methods

2.1. Identification and staining of specimens

Two *Epistylis* morphotypes adhered onto different aquaculture *Procambarus clarkia*. Morphotype I adhered onto the pereopods (sample number: 15) in Qianjiang City, Hubei Province, China (30°15′ N; 112°47′ E) on 28th April, 2016 and adhered onto the gills (sample number: 14) in Xiaogan City (31°01′ N; 113°50′ E) on 9th January, 2019. Morphotype II attached onto the pereopods of *P. clarkia* (sample number: 10) at the same pond of morphotype I in Qianjiang City (30°15′ N; 112°47’ E) on 8th May, 2016. Both morphotypes were treated by using the same methods as follows.

Life zooids were detached from the surface of hosts by using glass micropipettes under a dissecting microscope with the methods described by Wang et al. (2017a, b). The zooids were washed five to six times with distilled water to remove the salts. Observations of live specimens were conducted with bright-field and differential interference contrast microscopy (Olympus BX53F, Japan) at 200× to 1,000× magnifications. Images were captured by using a digital camera mounted to a microscope (Olympus DP73, Japan). The morphometric data were measured with a calibrated ocular attached to an optic microscope.

Protargol staining and silver nitrate methods (Foissner, 2014) were used to reveal infraciliature and pellicle striations respectively. Illustrations of live and stained specimens were drawn based on micrographs with Photoshop CS6 Extended (Adobe Systems Inc).

2.2. DNA extraction, polymerase chain reaction (PCR), and sequencing

Genomic DNA was extracted by using the TransDirect Animal Tissue PCR Kit (Trans, Beijing, China). The small subunit (SSU) rDNA, large subunit (LSU) rDNA and ITS1-5.8S-ITS2 were amplified, which were important maker for species identification used in sessilids (Jiang et al., 2016; Utz et al., 2010; Wang et al., 2017a, b). Small subunit (SSU) rDNA and large subunit (LSU) rDNA with the primers Euk A & Euk B (Medlin et al., 1988) and 28S–1F & 28S-3R (Moreira et al., 2007). The cycling parameters were as follows: 10 min initial denaturation at 95 °C, followed by 30 cycles (30 s at 95 °C for denaturation, 30 s at 55 °C for primer annealing and 1 min at 72 °C for extension) and a final extension step at 72 °C for 5 min. The entire ITS1-5.8S-ITS2 region was amplified with the primers ITSF and ITSR (Yi et al., 2009). The PCR program began with an initial denaturation step of 5 min at 95 °C, then followed by 30 cycles (1 min at 94 °C for denaturation, 30 s at 56 °C for annealing, 1 min at 72 °C for extension) and extension step of 72 °C for 7 min.

The PCR products were purified by using a High-Pure PCR Product Purification Kit (Cwbio, Beijing, China). High-pure fragments were inserted with pMD-19T-vector (Takara, Dalian, China), subsequently transforming target fragments into cells of *Escherichia* Trans-5α competent cells (Trans, Beijing, China). The samples were sequenced with an ABI PRISM® 3730 DNA sequencer (Applied Biosystems Inc., Foster City, CA, USA) by using the same primers as that for PCR.

2.3. Phylogenetic analysis

The genetic distances were performed by using MEGA. A blast search of the sequences of the two morphotypes and telotrochs was performed at https://blast.ncbi.nlm.nih.gov/Blast.cgi. Highly matched sequences were acquired from GenBank and aligned by using MAFFT v7.245 (Katoh and Standley, 2013). The alignment of SSU rDNA sequences and ITS1-5.8S-ITS2 sequences was trimmed by using GBLOCKS. The final alignment that was used for subsequent phylogenetic analyses included 1,579 sites for the SSU rRNA gene sequences and 156 sites for the ITS1-5.8S-ITS2 sequences. Phylogenetic trees were constructed by using Bayesian Inference (BI) and Maximum Likelihood (ML) methods. Bayesian analysis was performed with MrBayes 3.1.2. Markov chain Monte Carlo chains of SSU rDNA sequences and ITS1-5.8S-ITS2 sequences with default heating parameter for 1,000,000 generations, and trees were sampled every 100 generations with a burn-in of 2,500. Maximum likelihood (ML) trees were constructed with software PhyML 3.0 software under the best selected evolutionary model. Bootstrap percentages were obtained after 1000 replicates.

The best model (GTR + I + G) of nucleotide evolution analysis was selected by using the AIC criterion in jModeltest 2.1.10. The parameters of SSU rDNA sequences were as follows: nucleotide frequencies (A = 0.2949, C = 0.1801, G = 0.2437, T = 0.2813); substitution Rate matrix ([AC] = 1.3905, [AG] = 3.3688, [AT] = 1.7799, [CG] = 0.8711, [CT] = 5.6826, [GT] = 1.0000); proportion of invariable sites (I) = 0.3440; gamma distribution shape parameter = 0.5170. Furthermore, the best model for the ITS1-5.8S-ITS2 sequences was (GTR + I + G) with the following programmers: nucleotide frequencies (A = 0.3359, C = 0.1815, G = 0.1831, T = 0.2995); substitution rate matrix ([AC] = 1.6034, [AG] = 4.4271, [AT] = 2.0330, [CG] = 0.5475, [CT] = 5.3357, [GT] = 1.0000); proportion of invariable sites (I) = 0.281; gamma distribution shape parameter = 0.511.

3. Results

Genus *Epistylis* Ehrenberg, 1830.

***Epistylis semiciculus* n. sp.**

Host and site: pereopods and gills of *Procambarus clarkia*.

Prevalence and sampling sites: shown in Table 1.

Diagnosis. Extended zooids vase-shaped. Macronucleus C-shaped

Table 1
Sample information of two morphotypes.

Data	sample number	morphotypes	attachment-site	rate	intensity
28th April, 2016	15	I	pereopods	100%	> 100
8th May, 2016	10	II	pereopods	100%	> 100
9th January, 2019	14	I	gill	7%	20

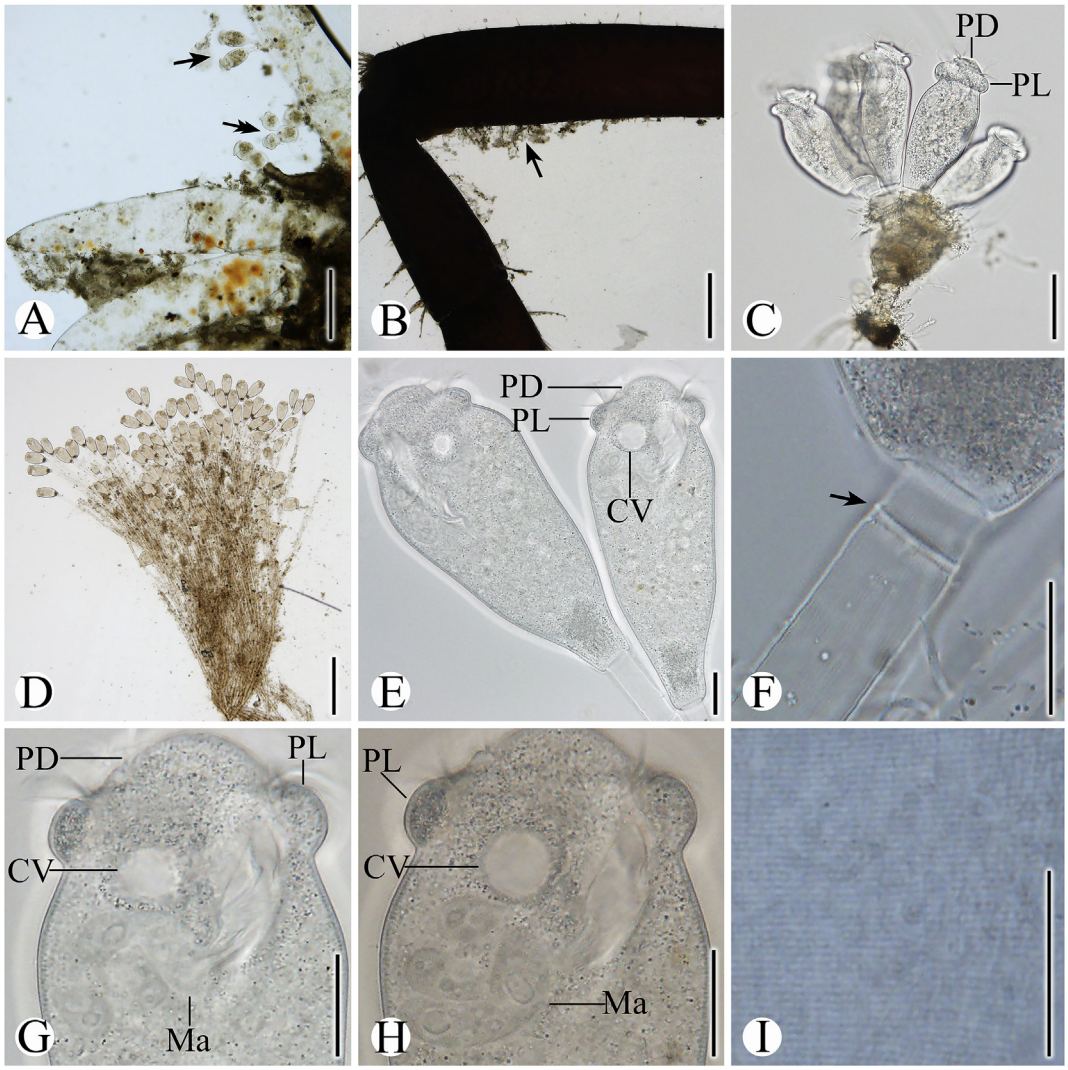

Fig. 1. *Epistylis semiciculus* n. sp. in vivo. **A**. Morphotype I stick to the gill of *P. clarkia*, double arrow shows *Carchesium* sp., arrow shows the zooids of Poulation I. **B**. Morphotype II stick to the pereopods of *P. clarkia*, arrow shows the zooids of Poulation II. Uncontracted zooids of morphotype I. **C**. Colony of morphotype I. **D**. Colony of Morphotype II. **E.** Uncontracted zooids of Morphotype II. **F**. Stalk, arrow shows the transverse striation. **G, H.** Macronucleus. **I.** Transverse striations on pellicle. ATB, aboral trochal band; CV, Contractile vacuole; Ma, macronucleus; PD, peristomial disk; PL, peristomial lip. Scale bars: A = 200 μm; B = 3 mm; C = 40 μm; D = 400 μm; E, F, G, H, I = 20 μm.

Table 2
Morphometric data of *Epistylis semiciculus* n. sp. (all measurements in μm).

Characters	Population	n	Min	Max	Mean	SD	CV	P
zooid length, in vivo	I	13	78.9	103.8	87.6	7.05	8.05	0
	II	18	136.7	171.5	153.8	10.05	6.39	
Zooid Width	I	13	32.1	54.6	42.1	5.96	13.97	0
	II	18	60.9	88.0	73.6	6.04	8.45	
Stalk Width	I	7	9.6	14.5	11.9	1.76	14.78	0.966
	II	12	9.0	13.9	11.6	1.52	13.11	
Secondary stalk length	I	10	34.3	50.0	42.5	5.48	12.88	0
	II	10	2048.1	2424.1	2278.5	135.25	5.93	
Peristomial Disk diameter	I	10	17.8	21.7	19.7	1.39	7.06	0
	II	10	30.2	37.9	33.3	2.12	6.36	
Peristomial Disk height	I	10	5.0	9.2	7.2	1.48	20.67	0
	II	10	9.6	13.9	11.1	1.62	14.57	
Peristomial Lip diameter	I	10	30.8	35.5	41.1	6.85	16.5	0
	II	10	54.3	62.5	57.1	2.75	4.82	
Peristomial lip height	I	10	8.2	11.6	9.6	1.14	11.89	0.001
	II	10	10.3	15.5	13.1	1.65	12.59	
Silver line	I	10	152	195	172	12.69	7.38	0.88
	II	12	177	238	196	18.70	9.50	

I, morphotype I collected on April 28th, 2016 and 9th January, 2019; II, morphotype II collected on May 8th, 2016; n, number of specimens measured; Min, Minimum; Max, Maximum; Mean, arithmetic mean; SD, standard deviation; CV, coefficient of variation in %; P, P value.

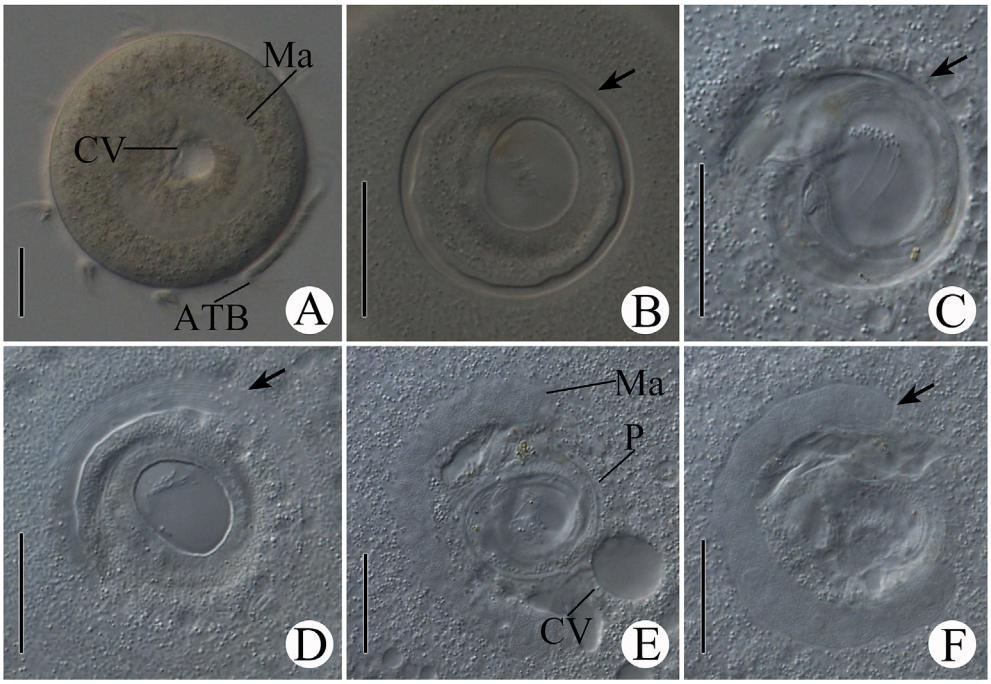

Fig. 2. Telotrochs of morphotype II of *Epistylis semiciculus* n. sp. in vivo. **A**. Apical view of telotroch. **B**. Oral of telotroch (arrow). **C**. Oral infraciliature (arrow). **D**. Transverse striations on oral pellicle (arrow). **E.** Macronucleus and infraciliature. **F.** Macronucleus (arrow). ATB, aboral trochal band; CV, Contractile vacuole; Ma, macronucleus; P, polykinety. Scale bars = 10 μm.

with variable orientation. One contractile vacuole ventrally located below peristomial lip. Number of silverlines 152–238 from peristome to scopula. Three rows of P1 equaled in length. Three rows of P2 terminate at same level. The inner row of P3 shorter than other the two rows.

3.1. Type locality

Morphotype I was found in freshwater crayfish pond in Qianjiang City (30°15′ N; 112°47′ E) and Xiaogan City (31°01′ N; 113°50’ E), Hubei Province, China.

Morphotype II was found in freshwater crayfish pond in Qianjiang City (30°15′ N; 112°47’ E), Hubei Province, China.

Type material: The protargol-stained slide containing the holotype specimen and the silver nitrate strained slide containing the paratype have been deposited in the National Zoological Museum of China, Institute of Zoology, Chinese Academy of Sciences, Beijing, China, with registration number HB2016001 and HB2016002. Three protargol-stained slides have been deposited in the Department of Aquatic Animal Medicine, College of Fisheries, Huazhong Agricultural University, Wuhan, China, with registration number zt201604281, zt201604282 and zt201604283.

Etymology: The species-group name *Epistylis semiciculus* refers to the semicircular peristomial disk.

3.2. Description

Morphotypes I detected adhering onto the pereopods and the gills of *Procambarus clarkia* (Fig. 1A). Colonies consisted of 4–6 zooids (Figs. 1C and 4A) with extremely short secondary stalks (mean length 43 μm) (Fig. 1C). Zooids measured 80–105 × 30–55 (average 87.6 × 42.6) μm with length-to-width radio of 2:1 (Fig. 1C). Secondary stalk average 42.5 μm in length (Fig. 1C). Peristomial lip average 9.6 (8.2–11.6) μm in thickness and 41.1 (30.8–35.5) μm in diameter. Peristomial disk 19.7 (17.8–21.7) μm in diameter, and evidently elevated above peristome at a height of 7.2 (5.0–9.2) μm (Table 2). Numerous granules were distributed uniformly in the zooids (Fig. 1C).

Morphotype II adhered onto the pereopods of *Procambarus clarkia* (Fig. 1B). Colonies approximately consisted of 90 zooids (Figs. 1D and 4B). The expanded zooids measured 135–170 × 60–90 (153.8 × 73.6) μm (Figs. 1E and 4C) with average length-to-width radio of 2:1. Secondary stalk averaged 2278.5 μm in length (Fig. 1D). Peristomial lip, measured 57.1 (54.3–62.5) μm in diameter and 13.1 (10.3–15.5) μm in thickness (Fig. 1E). Peristomial disk measured 33.3 (30.2–37.9) μm in diameter with an average height of 11.1 (9.6–13.9) μm (Table 2). The cytoplasm near the scopula was darker than that of the other regions because of different density of gray granules (Fig. 1E).

Despite the morphometry and granules, the two morphotypes presented congruent morphological characteristics. Zooids presented a vase-shaped body (Fig. 1C, E). Peristomial disk revealed semicircle-shaped and evidently elevated above peristomial lip (Fig. 1G and H). Shallow longitudinal and obvious transverse striations visible on stalk surface (Fig. 1F). Single contractile vacuole dorsally located blow peristomial lip (Fig. 1E). C-shaped macronucleus located at anterior body with longitudinal (48% zooids, Fig. 1G) or transverse (52% zooids, Fig. 1H) orientation. Transverse striations were clearly visible on pellicle at ×1000 magnification (Fig. 1I).

Zooids detected leaving stalk and transforming free-swimming form (telotrochs). Body shape of telotrochs slightly similar to that of mobilids in morphology (Fig. 2A). C-shaped macronucleus oriented at center zooids (Fig. 2E and F). Oral infraciliature (Fig. 2B and C) and transverse striations detected on oral region at ×1000 magnification (Fig. 2D). Individual telotroch can swim by using cilia (Fig. 2A).

Macronucleus presented C-shaped with transverse or longitudinal orientation after protargol strained (Fig. 3B and C) and silver impregnated (Fig. 3I). Aboral trochal band revealed at anterior 65% of zooid length (Fig. 3C). Oral infraciliature of the two morphotypes was identical after protargol straining (Figs. 3A and 4D). Polykinety (P) turned 1.5 times around peristomial disk with the hapokinety (H). Germinal kinety emerged at distal end of polykinety and hapokinety (Figs. 3A and 4D). Polykinety transformed into infundibular polykinetids 1–3 (P1–3) within infundibulum (Fig. 3A). Three rows of P1 equaled in length (Fig. 3A, D). Three rows of P2 terminated at same level (Fig. 3E and F). Inner row of P3 shorter other equal two rows (Fig. 3E and F). After dry silver impregnated, transverse silverlines (Fig. 3G and H, 4E) and pores (Figs. 3G and 4E) detected on pellicle. The average numbers of silverlines from peristome to scopula 172 (morphotype I) and 196 (morphotype II).

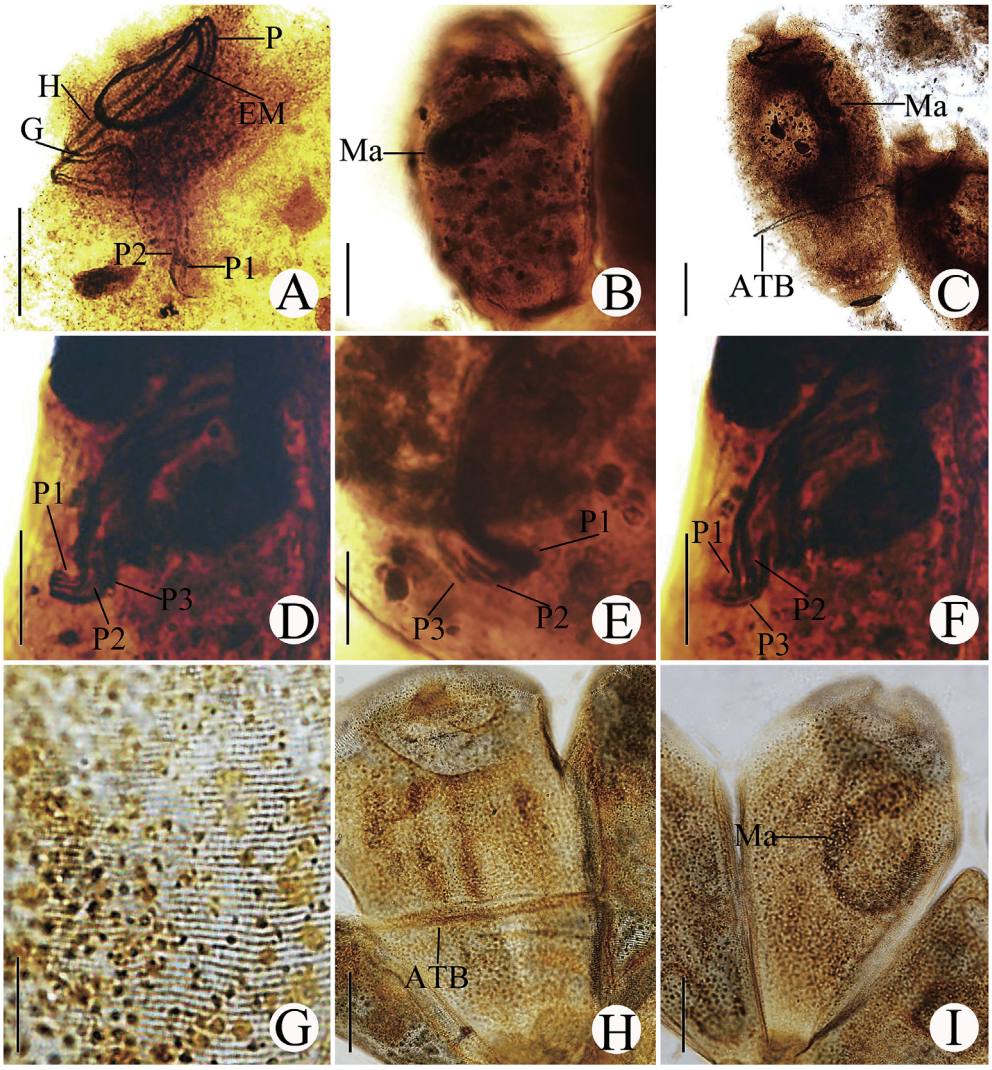

Fig. 3. Microphotographs of stained *Epistylis semiciculus* n. sp. with protargol stain (A–F) and silver nitrate (G–I). **A**. Pattern of infraciliature. **B.** Macronucleus with transverse orientation. **C**. Macronucleus with longitudinal orientation. **D, E, F**. Terminate of infundibular polykineties 1–3. **G, H**. Silver nitrate impregnated transverse striations, arrow shows the pores. I. Macronucleus after silver nitrate impregnated. ATB, aboral trochal band; G, germinal kinety; H, haplokinety; P, polykinety; P1–3, infundibular polykineties 1–3. Scale bars: A, B, C, H, I = 20 μm; D, E, F = 10 μm; G = 5 μm.

3.3. Sequence and phylogenetic analysis

Four SSU rDNA sequences of *Epistylis semiciculus* n. sp. were collected as follows: S1.1, S1.2 (from morphotype I, GenBank accession number: XXXX, XXXX), S2 (from morphotype II, GenBank accession number: XXXX), and S3 (telotrochs of morphotype II, GenBank accession number: XXXX). The length of all sequences was 1732 bp. Four sequences were aligned with each other and other available sequences in GenBank. The BLAST results and genetic distance were showed in Table 3. The identities between the two morphotypes (99.7–99.9% over 1730 bp) were higher than other sequences of single species (*E. plicatilis*, 99.6% over 1049 bp). The most similar available species was *E. portoalegrensis* (KT358502, 99.0–99.2% over 1612 bp) based on BLAST results. The ML and BI trees based on SSU rDNA sequences were almost congruent with respect to topologies. Thus, a single tree was shown based on the topology of BI tree with node support from both analyses revealed on the branches (Fig. 5). The phylogenetic tree revealed that the four sequences of *E. semiciculus* n. sp. grouped together within a well-supported clade (100 ML, 100BI), and clustered with major *Epistylis* that encompassed species of *E. portoalegrensis* (KT358502), *E. chrysemydis* (KM096378, AF335514), *E. chlorelligerum* (KM096377, KM096375), *E. wenrichi* (AF335515) and *E. urceolata* (AF335516). The clade of Epistylidae was sister to part species of *Zoothamnium*, such as *Z. sinca* (DQ190469), *Z. duplicatum* (DQ662851), *Z. nii* (DQ662852), *Z. arcuatum* (KM887953), and *Z. grossi* (KM887954).

Four ITS1-5.8S-ITS2 sequences were obtained as follows: I1 (from morphotype I, GenBank accession number: XXXX), I2.1, I2.2 (from morphotype II, GenBank accession number: XXXX, XXXX), and I3 (from telotrochs of morphotype II, GenBank accession number: XXXX). The length of all sequences was 495bp. BLAST results and genetic distances showed in Table 4. Blast results showed that similarities between the two morphotypes (99.8–100% over 495 bp) were higher than some different sequences of single species (*E. portoalegrensis*, 99.8% over 531 bp). Bayesian Inference (BI) and Maximum Likelihood (ML) trees based on ITS1-5.8S-ITS2 sequences provided consistent and strong supported topologies, and the congruent tree reconstructed together based on BI trees. Four sequences of *E. semiciculus* n. sp. clustered in a well-supported clade (96 ML, 100 BI), further nested with *E. portoalegrensis* (KT358504), *E. chrysemydis* (AF429887, GU586187), *E. urceolata* (AF429891) and *E. wenrichi* (AF429892), which clustered into a clade within Epistylididae (Fig. 6).

Collected LSU rDNA sequences were as follows: L1.1, L1.2 (from morphotype I, GenBank accession number: XXXX, XXXX), L2 (from morphotype II, GenBank accession number: XXXX), L3 (from telotrochs

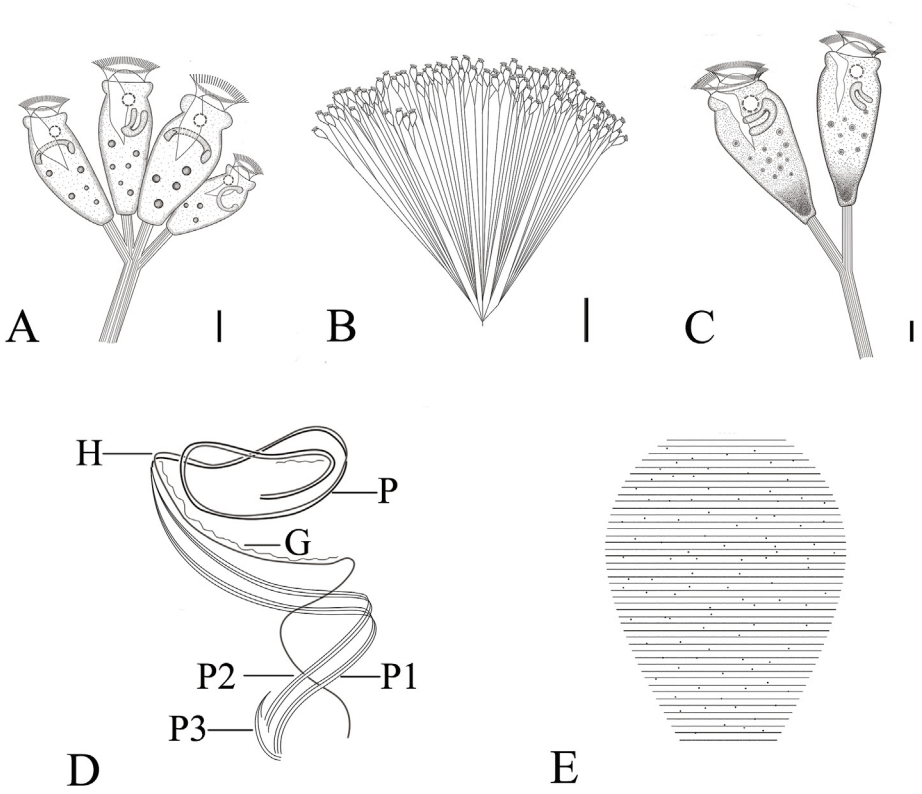

Fig. 4. *Epistylis semiciculus* n. sp. drawing from vivo and stained specimens. **A**. Morphotype I of *Epistylis semiciculus* n. sp. in vivo. **B, C**. Morphotype II of *Epistylis semiciculus* n. sp. in vivo. **D**. Oral infraciliature Oral. **E**. Transverse striations. G, germinal kinety; H, haplokinety; P, polykinety; P1–3, infundibular polykineties 1–3. Scale bars: A = 20 μm; B = 400 μm; C = 20 μm.

Table 3
SSU rDNA gene sequences genetic substitutions/genetic distance in bracket (lower triangle) and identities/nucleotides (upper triangle) among *Epistylis* species.

	1	2	3	4	5	6	7	8	9
1. S1.1		99.8%/1732	99.7%/1732	99.8%/1732	99.0%/1612	98.8%/1727	98.9%/1732	97.4%/1048	97.4%/1052
2. S1.2	4/0.002		99.9%/1732	100%/1732	99.2%/1612	99.0%/1727	99.1%/1732	97.7%/1048	97.7%/1052
3. S2	5/0.003	1/0.001		99.9%/1732	99.1%/1612	99.0%/1727	99.0%/1732	97.7%/1048	97.7%/1052
4. S4	4/0.002	0/0.000	1/0.001		99.2%/1612	99.0%/1727	99.1%/1732	97.7%/1048	97.7%/1052
5. E. portoalegrensis KT358502	17/0.011	13/0.008	14/0.009	13/0.008		99.50%/1612	99.4%/1613	97.1%/1051	97.1%/1055
6. *E. chrysemydis* AF335514	21/0.011	17/0.009	18/0.009	17/0.009	8/0.005		99.5%/1729	97.2%/1051	97.2%/1051
7. *E. chlorelligerum* KM096375	20/0.012	16/0.009	17/0.010	16/0.009	9/0.005	8/0.005		97.5%/1051	97.5%/1051
8. *E. plicatilis* HM627236	23/0.025	24/0.022	24/0.022	24/0.022	31/0.027	30/0.026	26/0.023		99.6%/1050
9. *E. plicatilis* HM627235	27/0.024	24/0.021	24/0.021	24/0.021	31/0.026	30/0.025	26/0.022	4/0.003	

Kimura 2 was used to calculate genetic distances.

of morphotype II, GenBank accession number: XXXX). Sequences length was 1843 bp, and the variant of different morphotypes was as follows: L1.1 differed from L1.2, and L3 by 2 substitutions (99.9% over 1843bp), 2 substitutions (99.9% over 1843bp), and 3 substitutions (99.8% over 1843 bp). L2 differed from L1.2, and L3 by 2 substitutions (99.9% over 1843 bp) and 5 substitutions (99.7% over 1843 bp). Phylogenetic tree was not constructed based on LSU rDNA sequences because only few sequences in GenBank were available.

4. Discussion

The present study presented morphological and molecular data of two sessilid morphotypes isolated from *Procambarus clarkia*, which will provide a reliable basis for pathogenic diagnosis. In addition, we demonstrated the two morphotypes are actually a single species based on almost similar morphological characteristics and molecular data, although the smaller and larger morphotypes showed distinct size ranges and granules. The species in the present study were identified as new species in genus *Epistylis*.

4.1. Expanded list of pathogenic ciliates on crustacean

Sessilids have repeatedly been reported adhering to edible crustacean during the late-20th century, causing potential damage to host health (López-Téllez et al., 2009). Many sessilids species were detected adhereing to crustacean in China, American, and Mexico, such as *Zoothamunium*, *Vorticella* and *Epistylis* (Hunn, 1966; Song et al., 1991; Hongwei and Overstreet, 2006; Liao et al., 2018). In the present study, we detected sessilids adhering onto intermolt period *Procambarus clarkia* tissues. Morphotype I and morphotype II were detected sticking to *P. clarkia* pereopods in spring (April and May), forming a filamentous layer over the surface, which may influence the movement of the host (Hunn, 1966; Villarreala and Hutchingsb, 1986). Moreover, morphotype I and *Carchesium* sp. firmly adhered onto the gills in winter (January), which was thought to reduce the effective respiratory surface area and increase respiratory stress for host in aquaculture condition (Overstreet, 1973). Considering the variable impact on different tissues, we suggested that the attachment-site preference under different environments should be carefully considered for the treatment of sessilinasis. To our best knowledge, this study is the first to describe sessilids isolated from *P. clarkia*, which may help aquaculturists for pathogenic

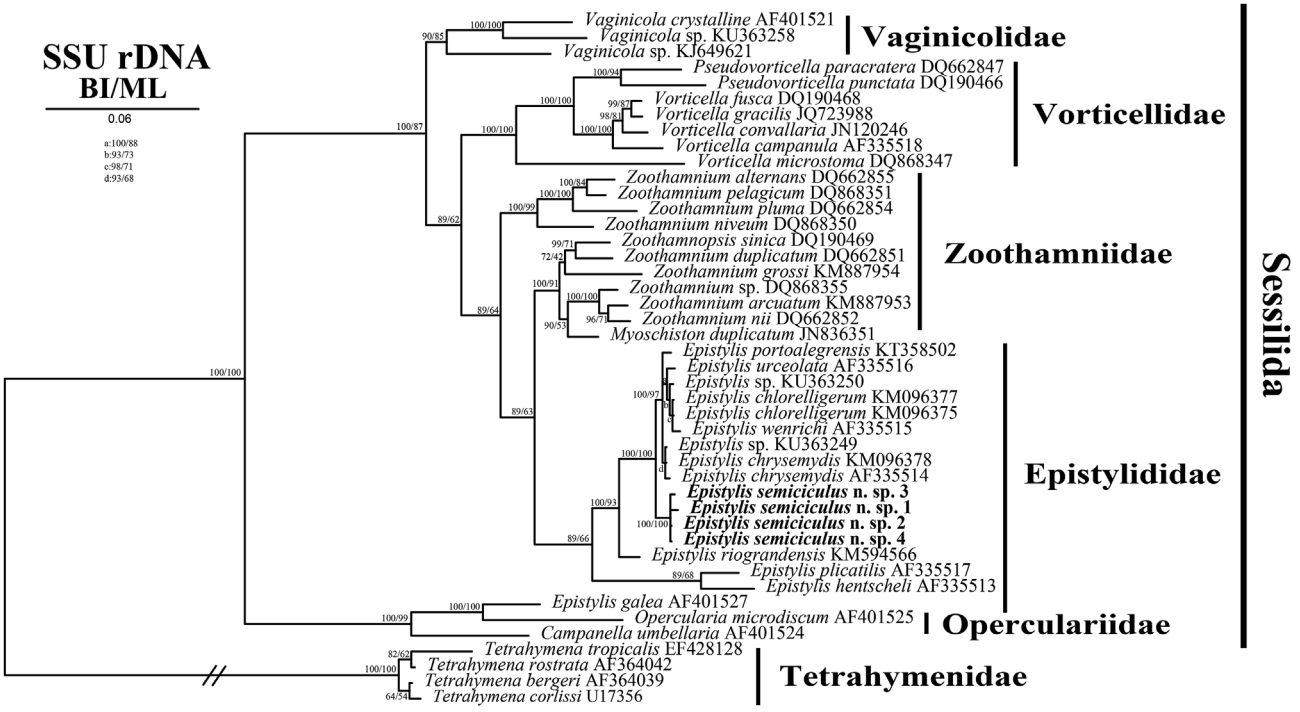

Fig. 5. Consensus tree constructed from both trees generated by phylogenetic analyses of nuclear SSU rDNA sequences. The sequences investigated in the present study are formatted in bold. Numbers at nodes of branches indicate the posterior probability (BI) and bootstrap (ML) values, respectively. 1 and 2, morphotype I; 3, morphotype II; 4, Telotrochs of morphotype II.

Table 4
ITS1-5.8S-ITS2 rDNA gene sequence substitutions/genetic distance (lower triangle) and identities/nucleotides (upper triangle) among *Epistylis* species.

	1	2	3	4	5	6	7	8
1. I1		99.8%/495	100%/495	99.6%/495	95.6%/481	95.8%/481	97.40%/194	97.9%/194
2. I2.1	1/0.002		99.8%/495	99.4%/495	95.4%/481	95.6%/481	96.70%/194	97.4%/194
3. I2.2	0/0.000	1/0.002		99.6%/495	95.6%/481	95.8%/481	96.40%/194	97.9%/194
4. I3	2/0.004	3/0.006	2/0.004		95.2%/481	95.4%/481	96.90%/194	97.4%/194
5. *E. portoalegrensis* KT358504	21/0.039	22/0.041	21/0.039	23/0.044		99.8%/531	98.4%/248	98.0%/249
6. *E. portoalegrensis* KT358503	20/0.037	21/0.039	20/0.037	22/0.041	1/0.002		98.4%/248	98.0%/249
7. *E. chrysemydis* AF429887	5/1.008	5/1.008	5/1.008	6/0.977	4/0.977	44/0.038		98.7%/385
8. *E. wenrichi* AF429892	4/0.993	5/0.993	4/0.993	5/0.963	5/0.008	5/0.008	5/0.008	

Kimura 2 was used to calculate genetic distances.

diagnosis and improve our understanding of the species diversity of sessilids isolated from crustaceans.

4.2. Comparison within conspecific

The two morphotypes in the present study were assigned to genus *Epistylis* based on their morphological characteristics, such as the colony without contractile stalks and the obvious peristomial lip. Morphologically, the two morphotypes both possessed a vase-shaped body, a semicircular peristomial disk, apically positioned contractile vacuole, variable macronucleus, and the same oral infraciliature, which are widely recognized as discriminating characteristics with obvious interspecies variations (Foissner et al., 1992; Jiang et al., 2016). However, number of zooids in colony, morphometric data and granules between the two morphotypes were significant different.

To solve the morphological conundrum above, molecular regions, including SSU rDNA, LSU rDNA, and ITS1-5.8S-ITS2 sequences were used for further identification. The result showed that the two morphotypes present very similar sequences with only 1 to 5 substitutions (SSU rDNA sequences, genetic distances: 0.06% to 0.29%), 2 substitutions (LSU rDNA sequences, genetic distances: 0.11%), and 0 to 1 substitution (ITS1-5.8S-ITS2 sequences, genetic distances: 0% to 0.20%) from each other. These molecular variations varied less than the other described conspecific morphotypes of *Epistylis* and other sessilids, with genetic distances ranging from 0.13% to 0.92% (Wu et al., 2011; Sun et al., 2012; Jiang et al., 2016). For example, the SSU rDNA sequences of *E. chrysemydis* vary 8 substitutions (genetic distances 0.53%, AF335514 vs. KY675178) and SSU rDNA sequences of *E. plicatillis* vary 5 substitutions (genetic distances 0.38%, HM627236 vs. HM627235). Moreover, phylogenetic analyses based on SSU rDNA sequences and ITS1-5.8S-ITS2 sequences both revealed that the two morphotypes belonged to a well-supported clade, which separate from other *Epistylis* species. Considering the similarities in molecular sequences and the fact that intraspecific morphological variation is common in peritriches (Jiang et al., 2016; Kühner et al., 2016; Marcotegui et al., 2018), the two morphotypes were identified to be conspecific. The morphological differences may be attributed to ontogenetic changes.

The commonly accepted morphological taxonomy within genus *Epistylis* and other sessilids include the following characteristics: body shape and size, infraciliature, silverlines, macronucleus, contractile vacuole, and granules (Lynn, 2008). However, precise identification of sessilids only based on morphology is quite difficult because of intraspecific morphological variations (Jiang et al., 2016; Kühner et al., 2016). In the present study, granules and body size were significantly

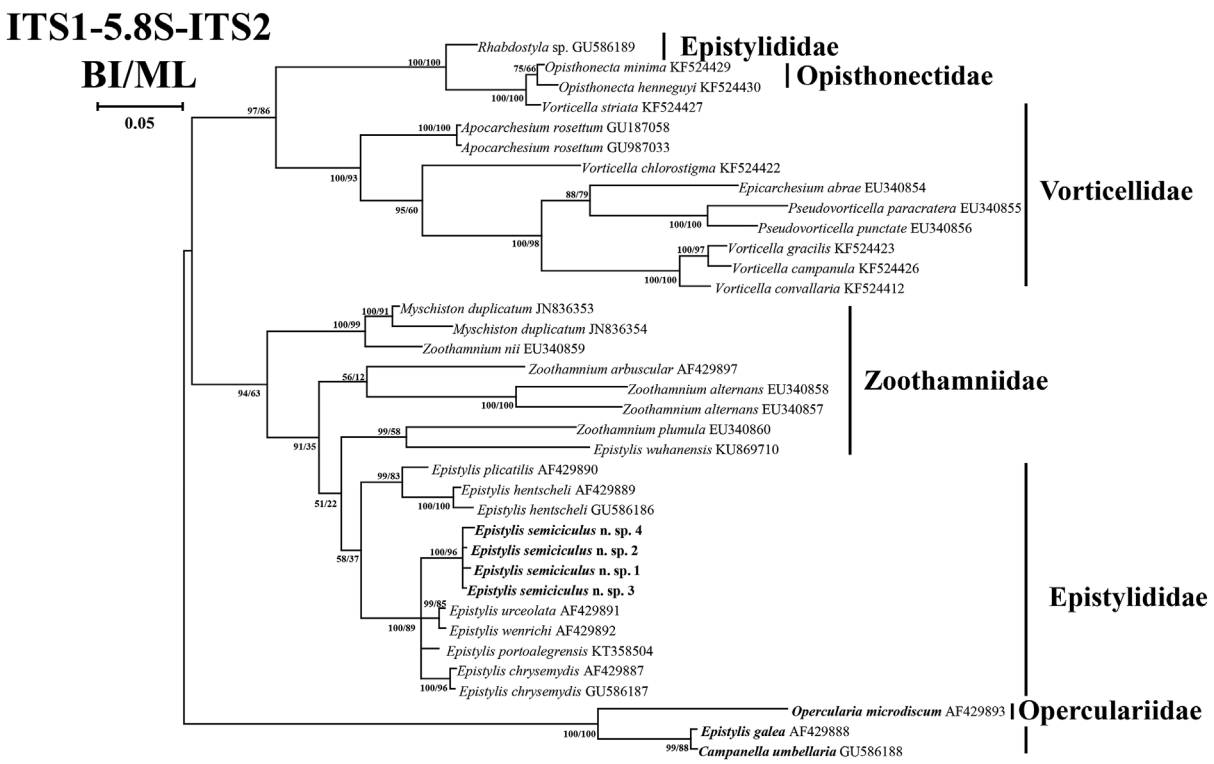

Fig. 6. Consensus tree constructed from both trees generated by phylogenetic analyses of nuclear ITS1-5.8S-ITS2 sequence. The sequences investigated in the present study are in bold. Numbers on branches indicate the posterior probability (BI) and bootstrap (ML) values, respectively. 1, morphotype I; 2 and 3, morphotype II; 4, Telotrochs of morphotype II.

different between the two morphotypes, which is consistent with previous studies, such as variable granules in cytoplasm of *E. chorelligerum*, and significant different body size of *E. wuhanensis* and *E. portoalegrensis* (Jiang et al., 2016; Kühner et al., 2016; Wang et al., 2017b). Moreover, the orientation of macronucleus of both morphotypes was variable in different zooids. These findings further verified the deficiency of some morphological characteristics used in species identification, such as body size and granules (Jiang et al., 2016; Wang et al., 2017b). These results highlighted the importance of molecular data for sessilid identification and pathogenic diagnosis (Miao et al., 2004; MartínCereceda et al., 2007; Gentekaki et al., 2017; Liao et al., 2018). The present study acted as a case for precise identification of sessilids from *Procambarus clarkia*: more data, especially comprehensive molecular data, should be considered when morphological identifying getting into dilemma.

4.3. Comparison with other Epistylis

The present species shows the typical morphological characteristics of the genus *Epistylis* and can be distinguished from other sessilid genera by the following typical morphological characteristics: noncontractile stalk, well-defined peristomial lip, and oral ciliary rows circling for less than two turns around peristomial disk (Lynn, 2008).

The present *Epistylis* can be distinguished from other *Epistylis* species by the following morphological characteristics: (1) body shape of several species is not vase shape, such as *E. aselli* Stiller, 1941, *E. gammari* Precht, 1935, *E. helicostylum* Vavra, (1962) and *E. hentscheli* Kahl, (1935) (vs. body shape of the present *Epistylis* is vase shape (Vavra, 1962; Foissner et al., 1992; Shen and Gu, 2016); (2) peristomial lips of several species are double layer, such as *E. chrysemydis* Bishop and Jahn, 1941 and *E. clampi* Hongwei and Overstreet, 2006 (vs. peristomial lip of the present *Epistylis* is single layer) (Hongwei and Overstreet, 2006; Jiang et al., 2016); (3) contractile vacuoles of several species are on the ventral wall of infundibulum, such as *E. acuminata* Song, 1986, *E. chlorelligerum* Shen, 1980 and *E. nympharum* Engelmann, 1862 (vs. contractile vacuole of the present *Epistylis* is on the dorsal wall of infundibulum) (Song, 1986; Foissner et al., 1992; Jiang et al., 2016); (4) peristomial disks of several *Epistylis* species are gradient, such as *E. chlorelligerum* and *E. vaginula* Stokes, 1884 (vs. peristomial disk of present *Epistylis* is semicircular) (Jiang et al., 2016; Shen and Gu, 2016) (5) contractile vacuole of several species are above peristomial lip, such as *E. acuminata*, *E. aselli*, *E. clampi*, *E. harpaticola* Kahl, 1933, *E. plicatilis* Ehrenberg, 1838 and *E. vaginula* (vs. contractile vacuole of the present *Epistylis* is below peristomial lip) (Song, 1991; Hong and Overstreet, 2006; Shi et al., 2014; Shen and Gu, 2016; (6) macronuclei of several species are J-shaped or band-shaped, such as *E. elongata* Stokes, 1889 and *E. nympharum* (vs. macronucleus of the present *Epistylis* is C-shaped) (Kahl, 1935; Foissner et al., 1992). Detailed comparisons are presented in Table 5.

The BLAST results show that the present *Epistylis* is most similar to *E. chlorelligerum* (KM096375, SSU rDNA sequences) and *E. chrysemydis* (GU586187, ITS1-5.8S-ITS2 sequences), which can be morphologically distinguished from the present *Epistylis* (see above). Phylogenetic analyses based on SSU rDNA sequences and ITS1-5.8S-ITS2 sequences both revealed that the present *Epistylis* obviously separates from other *Epistylis* species. Therefore, we identified the present *Epstylis* as a new species based on both morphological and molecular comparisons. We assigned it the name *Epistylis semiciculus* n. sp. with respect to the shape of its peristomial disk.

5. Conclusion

We presented morphological and molecular data of sessilids isolated from *Procambarus clarkia* for the first time. The comprehensive descriptions, including in vivo morphology, oral infraciliature, silverlines, and molecular data, will provide a reliable basis for pathogenic diagnosis. These results re-evolved the validity of some morphological characteristics as taxonomic criterion within sessilid, which highlighted the importance and convenience of molecular data on precise

Table 5
Morphological comparison of *Epistylis semiciculus* n. sp. with similar species.

Characteristic	*E. semiciculus*	*E. acuminata*	*E. aselli*	*E. chlorelligerum*	*E. clampi*	*E. chrysemydis*	*E. elongata*	*E. gammari*	*E. harpaticola*	*E. helicostylum*	*E. hentscheli*	*E. nympharum*	*E. plicatilis*	*E. vaginula*
Body shape	vase shape	funnel shape	funnel shape	vase shape	vase shape	vase	vase shape	ovalis shape	funnel shape	funnel shape	funnel shape	vase shape	funnel shape	funnel shape
PL layer	single	single	single	single gradient	double gradient	double	single	single semicircular	single	single	single	single	single gradient	single gradient
PD shape	semicircular	–	–	gradient	gradient	–	–	semicircular	–	–	–	–	gradient	gradient
CV location	dorsal, below PL	ventral, above PL	dorsal, above PL	ventral, below PL	dorsal, above PL	ventral, below PL	–	-, below PL	dorsal, above PL	-, below PL	ventral, below PL	ventral, below PL	dorsal, above PL	dorsal, above PL
Ma shape	C shape	C shape	C shape	C shape	C shape	C shape	band shape	C shape	C shape	band shape	C shape	J shape	C shape	C shape
Ma orientation	variable	transverse	transverse	transverse	transverse	transverse	longitudinal	transverse	transverse	longitudinal	transverse	longitudinal	transverse	transverse
Oral feature	H and P 1.5 turns; P1, three rows equal; P2, three rows equal; P3, three rows not equal	P1, three rows not equal	–	P2, two outer rows equal	H and P one circuit around PD	P3, three rows equal	–	–	–	–	–	–	P2, inner row shorter than two other rows	–
Stalk striations	transverse and longitudinal	–	–	longitudinal	longitudinal	longitudinal	–	transverse and longitudinal	transverse	–	transverse	–	no striation	longitudinal
Data source		Song (1986)	Shen and Gu (2016)	Jiang et al. (2016)	Ma and Overstreet (2006)	Jiang et al. (2016)	Kahl (1935)	Shen and Gu (2016)	Shen and Gu (2016)	Vavra (1962)	Foissner et al. (1992)	Foissner et al. (1992)	Shi et al. (2014)	Shen and Gu (2016)

Abbreviations: CV, contractile vacuole; H, haplokinety; P, polykinety; P1–3, infundibular polykineties 1–3; PD, peristomial disk; PL, peristomial lip; Ma, macronucleus; -, data are unavailable.

pathogenic diagnosis.

Declaration of competing interest

The authors declare that they have no competing interests.

Acknowledgements

This study was supported by Technical Innovation Project of Hubei Province (No. 2018ABA103) and Hubei Agricultural Science and Technology Innovation Center (2016620000001046).

Appendix ASupplementary data

Supplementary data to this article can be found online at https://doi.org/10.1016/j.ijppaw.2019.09.006.

References

Chen, L.S., Li, Y.S., Liu, Q.G., 2008. Ecological aquaculture of *Procambarus clarkia:* Chinese economics of *P. clarkia*. Fisheries Science & Technology Information. 35, 278–285. https://doi.org/10.3969/j.issn.1001-1994.2008.06.011.

Ehrenberg, C.G., 1830. Beiträge zur Kenntniß der Organisation der Infusorien und ihrer geographischen Verbreitung, besonders in Sibirien. Abh. dt. Akad. Wiss. Berl. Jahr 1–88.

FAO, 2018. The State of World Fisheries and Aquaculture. Meeting the sustainable development goals, Rome.

Foissner, W., 2014. An update of basic light and scanning electron microscopic methods for taxonomic studies of ciliated protozoa. Int. J. Syst. Evol. Microbiol. 64, 271–292. https://doi.org/10.1099/ijs.0.057893-0.

Foissner, W., Berger, H., Kohmann, F., 1992. Taxonomische und ökologische Revision der Ciliaten des Saprobiensystems-Band II: peritrichida, Heterotrichida, Odontostomatida. Informationsberichte des Bayer. Landesamt fur Wasserwirtschaft 5–92, 1–502.

Gao, F., Huang, J., Zhao, Y., Li, L., Liu, W., Miao, M., Zhang, Q., Li, J., Yi, Z., El-Serehy, H.A., Warren, A., Song, W., 2017. Systematic studies on ciliates (Alveolata, Ciliophora) in China: progress and achievements based on molecular information. Eur. J. Protistol. 61. https://doi.org/10.1016/j.ejop.2017.04.009.

Gentekaki, E., Kolisko, M., Gong, Y., Lynn, D., 2017. Phylogenomics solves a long-standing evolutionary puzzle in the ciliate world: the subclass Peritrichia is monophyletic. Mol. Phylogenetics Evol. 106, 1–5. https://doi.org/10.1016/j.ympev.2016.09.016.

Gherardi, F., 2006. Crayfish invading Europe: the case study of *Procambarus clarkia*. Mar. Freshw. Behav. Physiol. 39, 175–191. https://doi.org/10.1080/10236240600869702.

Hobbs, H.H., Jass, J.P., Huner, J.A.Y.V., 1989. A review of global crayfish introductions with particular emphasis on two north American species. Crustaceana 56, 299–316. https://doi.org/10.1163/156854089X00275.

Hongwei, M.A., Overstreet, R.M., 2006. Two new species of *Epistylis* (Ciliophora: peritrichida) on the blue crab (Callinectes Sapidus) in the gulf of Mexico. J. Eukaryot. Microbiol. 53, 85–95. https://doi.org/10.1111/j.1550-7408.2005.00080.x.

Hunn, J.B., 1966. Two peritrichous ciliates from the gills of the blue crab. Chesap. Sci. 171–176. https://doi.org/10.1007/BF02854045.

Jiang, C., Shi, X., Liu, G., Jiang, Y., Warren, A., 2016. Morphology and molecular phylogeny of two freshwater peritrich ciliates, *Epistylis chlorelligerum* Shen 1980 and *Epistylis chrysemydis* Bishop and Jahn 1941 (Ciliophora, Peritrichia). J. Eukaryot. Microbiol. 63, 16–26. https://doi.org/10.1111/jeu.12243.

Kahl, A., 1935. Urtiere oder Protozoa I: wimpertiere oder Ciliate (Infusoria) 4 Peritricha und Chonotricha. Tierwelt Dtl 30, 651–886.

Katoh, K., Standley, D.M., 2013. MAFFT multiple sequence alignment software version 7: improvements in performance and usability. Mol. Biol. Evol. 30, 772–780. https://doi.org/10.1093/molbev/mst010.

Kühner, S., Simão, T.L., Safi, L.S., Gazulha, F.B., Eizirik, E., Utz, L.R., 2016. *Epistylis portoalegrensis* n. sp. (Ciliophora, Peritrichia): a new freshwater ciliate species from southern Brazil. J. Eukaryot. Microbiol. 63, 93–99. https://doi.org/10.1111/jeu.12252.

Liao, C.C., Shin, J.W., Chen, L.R., Huang, L.L.H., Lin, W.C., 2018. First molecular identification of Vorticella sp. from freshwater shrimp in Tainan, Taiwan. Int. J. Parasitol.: Parasites and Wildlife 7 (3), 415–422. https://doi.org/10.1016/j.ijppaw.2018.10.002.

López-Téllez, N.A., Vidal-Martínez, V.M., Overstreet, R.M., 2009. Seasonal variation of ectosymbiotic ciliates on farmed and wild shrimps from coastal Yucatan. Mexico. Aquaculture 287, 271–277. https://doi.org/10.1016/j.aquaculture.2008.11.003.

Lynn, D.H., 2008. The Ciliated Protozoa: Characterization, Classification, and Guide to the Literature. Springer, Dordrecht.

Marcotegui, P.S., Montes, M.M., Jorge, B., Walter, F., Sergio, M., 2018. Geometric morphometric on a new species of trichodinidae. a tool to discriminate Trichodinid species combined with traditional morphology and molecular analysis. Int. J. Parasitol.: Parasites and Wildlife 7, 228–236. https://doi.org/10.1016/j.ijppaw.2018.06.004.

MartínCereceda, M., Guinea, A., Bonaccorso, E., Dyal, P., Novarino, G., Foissner, W., 2007. Classification of the peritrich ciliate *Opisthonecta matiensis* (Martin-Cereceda et al. 1999) as *Telotrochidium matiense* nov. comb. based on new observations and SSU rDNA phylogeny. Eur. J. Protistol. 43, 265–279. https://doi.org/10.1016/j.ejop.2007.04.003.

Medlin, L., Elwood, H.J., Stickel, S., Sogin, M.L., 1988. The characterization of enzymatically amplified eukaryotic 16S-like rRNA-coding regions. Gene 71, 491–499. https://doi.org/10.1016/0378-1119(88)90066-2.

Overstreet, R., 1987. Solving parasite-related problems in cultured Crustacea. Int. J. Parasitol. 17, 309–318. https://doi.org/10.1016/0020-7519(87)90105-6.

Miao, W., Fen, W.S., Yu, Y.H., Zhang, X.Y., Shen, Y.F., 2004. Phylogenetic relationships of the subclass Peritrichia (Oligohymenophorea, Ciliophora) inferred from small subunit rRNA gene sequences. J. Eukaryot. Microbiol. 51, 180–186. https://doi.org/10.1111/j.1550-7408.2004.tb00543.x.

Moreira, D., Heyden, S.V.D., Bass, D., López-García, P., Chao, E., Cavalier-Smith, T., 2007. Global eukaryote phylogeny: combined small- and large-subunit ribosomal DNA trees support monophyly of Rhizaria, Retaria and Excavata. Mol. Phylogenet. Evol. 44, 255–266. https://doi.org/10.1016/j.ympev.2006.11.001.

Overstreet, R.M., 1973. Parasites of some penaeid shrimps with emphasis on reared hosts. Aquaculture 2, 105–140. https://doi.org/10.1016/0044-8486(73)90140-3.

Pádua, S.B.D., Ishikawa, M.M., Ventura, A.S., Jerönimo, G.T., Martins, M.L., Tavares, L.E.R., 2013. Brazilian catfish parasitized by *Epistylis* sp. (Ciliophora, Epistylididae), with description of parasite intensity score. Parasitol. Res. 112, 443–446. https://doi.org/10.1007/s00436-012-3069-5.

Shen, Y., Gu, M., 2016. Ciliophora, Oligohymenophorea, Peritrichida. Fauna Sinica, Invertebrata, vol. 45 Science press, Beijing.

Shi, X., Meng, Q.J., Liu, G.J., Qi, G.L., Jiang, C.Q., Meng, X.W., Warren, A., 2014. Morphology and morphogenesis of *Epistylis plicatilis*, Ehrenberg, 1831 (Ciliophora, peritrichia) from wuhan, China. J. Morphol. 275, 882–893. https://doi.org/10.1002/jmor.20265.

Song, W.B., 1986. Descriptions of seven new species of peritrichs on Penaeus orientalis (Peritricha: zoothamnidae, Epistylidae). Zoological Systematics 11, 225–234.

Song, W.B., 1991. A new coomensal ciliate, *Zoothamnium paraentzii* (Ciliophora, Perithichida). Zool. Res. 23, 90–94.

Sun, P., Clamp, J., Xu, D., Kusuoka, Y., Miao, W., 2012. *Vorticella* linnaeus, 1767 (Ciliophora, Oligohymenophora, Peritrichia) is a grade not a clade: redefinition of *Vorticella* and the families Vorticellidae and Astylozoidae using molecular characters derived from the gene coding for small subunit ribosomal RNA. Protist 163, 129–142. https://doi.org/10.1016/j.protis.2011.06.005.

Utz, L.R., Simao, T.L., Safi, L.S., Eizirik, E., 2010. Expanded phylogenetic representation of genera *Opercularia* and *Epistylis* sheds light on the evolution and higher-level taxonomy of peritrich ciliates (Ciliophora: peritrichia). J. Eukaryot. Microbiol. 57, 415–420. https://doi.org/10.1111/j.1550-7408.2010.00497.x.

Vavra, J., 1962. *Epistylis helicostylum* n. sp. a new peritrichous ciliate with an allometric stalk formation. J. Eukaryot. Microbiol. 9, 469–473. https://doi.org/10.1111/j.1550-7408.1962.tb02656.x.

Van, A.J.G., Viljoen, S.A., 1984. Taxonomic study of sessile peritrichs (Ciliophora: peritricha) associated with crustacean fish ectoparasites in South Africa. S. Afr. J. Zool. 19, 275–279. https://doi.org/10.1080/02541858.1984.11447893.

Villarreala, H., Hutchingsb, R.W., 1986. Presence of ciliate colonies on the exoskeleton of the freshwater crayfish *Cherax Tenuimanus* (smith) (Decapoda: Parastacidae). Aquaculture 58, 309–312. https://doi.org/10.1016/0044-8486(86)90097-9.

Vogelbein, W.K., Thune, R.L., 1988. Ultrastructural features of three ectocommensal protozoa attached to the gills of the red swamp crawfish, *Procambarus clarkia* (Crustacea: Decapoda). J. Eukaryot. Microbiol. 35, 8. https://doi.org/10.1111/j.1550-7408.1988.tb04103.x.

Wang, J.G., Feng, Y.M., Wang, Z., Gu, H.L., Lu, H.D., Wang, Q., 2016. The investigation of sessilinasis and efficacy of zinc sulphate to sessilinasis of *Procambarus clarkia*. Freshw. Fish. 46 50-49. https://doi.org/10.13721/j.cnki.dsyy.20160505.015.

Wang, Z., Zhou, T., Gu, Z., 2017a. New data of two trichodinid ectoparasites (Ciliophora: trichodinidae) from farmed freshwater fishes in Hubei, China. Eur. J. Protistol. 60, 50. https://doi.org/10.1016/j.ejop.2017.04.002.

Wang, Z., Zhou, T., Guo, Q., Gu, Z., 2017b. Description of a new freshwater ciliate *Epistylis wuhanensis* n. sp. (Ciliophora, Peritrichia) from China, with a focus on phylogenetic relationships within family Epistylididae. J. Eukaryot. Microbiol. 64, 394–406. https://doi.org/10.1111/jeu.12375.

Wu, S., Shi, X., Utz, L.R., Liu, G., Ji, D., Zhao, Y., Wang, H., 2011. Morphology and morphogenesis of a freshwater ciliate, *Epistylis chlorelligerum* Shen, 1980 (Ciliophora, Peritrichia). J. Eukaryot. Microbiol. 58, 120–127. https://doi.org/10.1111/j.1550-7408.2010.00528.x.

Xu, L.J., Lv, Y.H., 2018. China Fishery Statistical Yearbook. China Agriculture Press, Beijing.

Yi, Z., Song, W., Clamp, J.C., Chen, Z., Gao, S., Zhang, Q., 2009. Reconsideration of systematic relationships within the order Euplotida (Protista, Ciliophora) using new sequences of the gene coding for small-subunit rRNA and testing the use of combined data sets to construct phylogenies of the *Diophrys*-complex. Mol. Phylogenetics Evol. 50, 599–607. https://doi.org/10.1016/j.ympev.2008.12.006.